Application of the mean curvature flow in the image segmentation

A. Handlovičová, K. Mikula, M. Tibenský, T. Hornáček

Slovak Technical University in Bratislava
Differential Equations and Applications 2017

6. septembra 2017

Content of the presentation

A. Handlovičová, K. Mikula, M. Tibenský, T. Horňáček

Image segmentation

The motivation is to study problems arising in the image segmentation and edge detection and to find new numerical scheme for solving it.

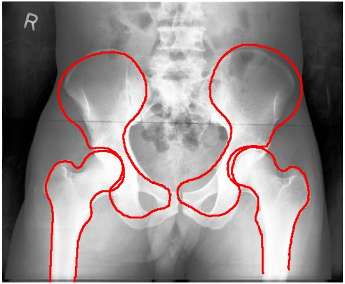

Eymard R., Handlovičová A., Mikula K.: *Study of a finite volume scheme for regularised mean curvature flow level set equation*. IMA Journal on Numerical Analysis, Vol. 31, 813-846, 2011.

Time dependent segmentation

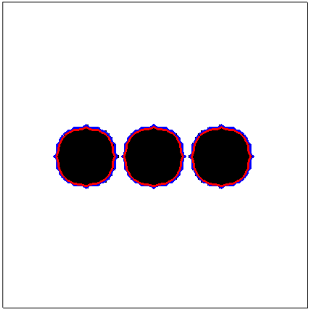

Hornacek T., Mikula K.: Numerical methods for 4D segemntation, STU, 2017.

Time dependent segmentation

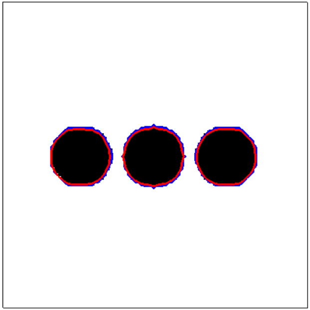

Hornacek T., Mikula K.: Numerical methods for 4D segemntation, STU, 2017.

Time dependent segmentation

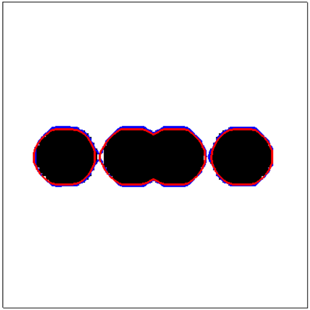

Hornacek T., Mikula K.: Numerical methods for 4D segemntation, STU, 2017.

Time dependent segmentation

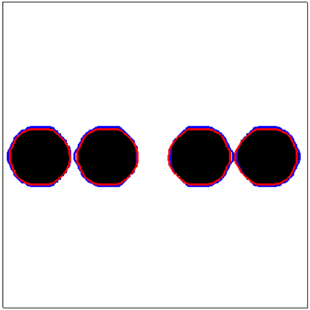

Hornacek T., Mikula K.: Numerical methods for 4D segemntation, STU, 2017.

Level set function

We construct the initial level set function and we are monitoring development of the isolines:

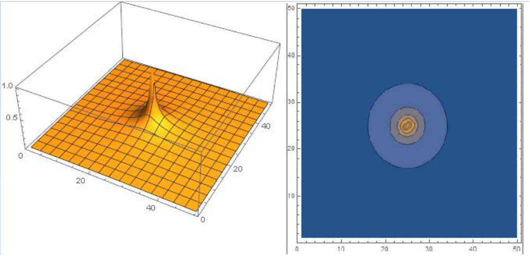

Obr.: Initial level set function

Osher S., Sethian J.: Fronts propagating with curvature dependent speed: algorithm based on Hamilton-Jacobi formulation,J.Comput. Phys., 79 (1988) pp. 12–49.

Principle of the level set approach

If we want to monitor isolines of the level set function u we have to monitor set of points such that $u(x,t) = c$ for $\forall x \in \Omega$ and $\forall t \in [0, T]$.
Then following equation has to be fulfilled:

$$0 = \frac{d}{dt}(u(x(t),t)) = \frac{\partial u}{\partial t} + \nabla u \cdot \dot{x}. \qquad (1)$$

Depending on selection of $\dot{x}$ we receive one of the following equations:

Mean curvature in the level set approach

1. Constant vector field: $\dot{x} = \overrightarrow{v}$:

$$\frac{\partial u}{\partial t} + \overrightarrow{v} \cdot \nabla u = 0.$$

2. Movement in the normal direction: $\dot{x} = \beta \overrightarrow{N} = \beta \frac{\nabla u}{|\nabla u|}$:

$$\frac{\partial u}{\partial t} + \beta \frac{\nabla u}{|\nabla u|} \cdot \nabla u = \frac{\partial u}{\partial t} + \beta |\nabla u| = 0.$$

3. Motion controlled by curvature: $\dot{x} = -\nabla \cdot \left(\frac{\nabla u}{|\nabla u|} \right) \frac{\nabla u}{|\nabla u|}$:

$$\frac{\partial u}{\partial t} - |\nabla u| \nabla \cdot \left(\frac{\nabla u}{|\nabla u|} \right) = 0.$$

This equation is called level set equation.

Content of the presentation

Studied equation

We introduce a semi-implicit numerical scheme for the equation

$$u_t - f(|\nabla u|)\nabla \cdot \left(g(|\nabla G_S * I^0|) \frac{\nabla u}{f(|\nabla u|)} \right) = r, \qquad (2)$$
$$a.e.\ (x,t) \in \Omega \times (0,T),$$

where $u(x,t)$ is an unknown (segmentation) function and I^0 is a given image. Functions g, f, G_S a r are given initial data of the problem.
We consider zero Dirichlet boundary condition

$$u = 0, \quad a.e.\ (x,t) \in \partial\Omega \times [0,T] \qquad (3)$$

and initial condition

$$u(x,0) = u_0(x), \quad a.e.\ x \in \Omega. \qquad (4)$$

Assumptions on the data

1. Function $f : \mathbb{R}_0^+ \to \mathbb{R}^+$ defined as $f(s) = \min(\sqrt{s^2 + a^2}, b)$, for $0 < a < b$, is the regularisation,

Assumptions on the data

1. Function $f : \mathbb{R}_0^+ \to \mathbb{R}^+$ defined as $f(s) = \min(\sqrt{s^2 + a^2}, b)$, for $0 < a < b$, is the regularisation,
2. $r \in L^2(\Omega \times (0, T))$ for all $T > 0$,

Assumptions on the data

1. Function $f : \mathbb{R}_0^+ \to \mathbb{R}^+$ defined as $f(s) = \min(\sqrt{s^2 + a^2}, b)$, for $0 < a < b$, is the regularisation,
2. $r \in L^2(\Omega \times (0, T))$ for all $T > 0$,
3. $G_S \in C^\infty(\mathbb{R}^d)$ is a smoothing kernel (Gauss function), such that $\int_{\mathbb{R}^d} G_S(x)dx = 1$, usually is used function $G_S(x) = \frac{1}{(4\pi S)^{d/2}} e^{-|x|^2/4S}$,

Assumptions on the data

1. Function $f : \mathbb{R}_0^+ \to \mathbb{R}^+$ defined as $f(s) = \min(\sqrt{s^2 + a^2}, b)$, for $0 < a < b$, is the regularisation,
2. $r \in L^2(\Omega \times (0, T))$ for all $T > 0$,
3. $G_S \in C^\infty(\mathbb{R}^d)$ is a smoothing kernel (Gauss function), such that $\int_{\mathbb{R}^d} G_S(x)dx = 1$, usually is used function $G_S(x) = \frac{1}{(4\pi S)^{d/2}} e^{-|x|^2/4S}$,
4. $\nabla G_S * I^0 = \int_{\mathbb{R}^d} \nabla G_S(x - \xi)\tilde{I^0}(\xi)d\xi$, where $\tilde{I^0}$ is an extension of the image I^0 to $\mathbb{R}^d$ given by periodic reflection through the boundary of Ω,

Assumptions on the data

1. Function $f : \mathbb{R}_0^+ \to \mathbb{R}^+$ defined as $f(s) = \min(\sqrt{s^2 + a^2}, b)$, for $0 < a < b$, is the regularisation,
2. $r \in L^2(\Omega \times (0, T))$ for all $T > 0$,
3. $G_S \in C^\infty(\mathbb{R}^d)$ is a smoothing kernel (Gauss function), such that $\int_{\mathbb{R}^d} G_S(x)dx = 1$, usually is used function $G_S(x) = \frac{1}{(4\pi S)^{d/2}} e^{-|x|^2/4S}$,
4. $\nabla G_S * I^0 = \int_{\mathbb{R}^d} \nabla G_S(x - \xi)\tilde{I}^0(\xi)d\xi$, where $\tilde{I}^0$ is an extension of the image I^0 to $\mathbb{R}^d$ given by periodic reflection through the boundary of Ω,
5. $g : \mathbb{R}_0^+ \to \mathbb{R}^+$ is decreasing function, $g(\sqrt{s})$ is smooth, $g(0) = 1$, $g(s) \to 0$ for $s \to \infty$, we are using function $g(s) = \frac{1}{1+Ks^2}$, $K \geq 0$.

Discretization of the problem

Discrete solution of our problem:

$$u_p^n \approx u(x_p, t) \tag{5}$$

for $t \in [n\tau, (n+1)\tau]$, $n = 1, ..., N_T + 1$ and $\forall p \in \mathcal{M}$.

Discretization of the problem

The approximation of the norm of the gradient:

$$N_p(u)^2 = \frac{1}{|p|} \sum_{\sigma \in \mathcal{E}_p} \frac{|\sigma|}{d_{p\sigma}} (u_\sigma - u_p)^2, \ \forall p \in \mathcal{M}, \ \forall u \in H_{\mathcal{D}}. \quad (6)$$

Discretization of the problem

Function g on the edge of the control volume:

$$g_\sigma^S := g^S(x_\sigma) = g(|\int_{\mathbb{R}^d} \nabla G_S(x_\sigma - \xi)\tilde{I^0}(\xi)d\xi|) \qquad (7)$$

or

$$g_p^S := \min_{\sigma \in \mathcal{E}_p} g_\sigma^S. \qquad (8)$$

Discretization of the problem

Numerical scheme of the studied problem based on EHM approach:

$$\frac{|p|\ (u_p^{n+1} - u_p^n)}{\tau\ f(N_p(u^n))} - \frac{1}{f(N_p(u^n))} \sum_{\sigma \in \mathcal{E}_p} g^S \frac{|\sigma|}{d_{p\sigma}} (u_\sigma^{n+1} - u_p^{n+1}) =$$

$$= \frac{r_p^{n+1}}{\tau\ f(N_p(u^n))}, \forall p \in \mathcal{M},\ \forall n \in \mathbb{N}, \tag{9}$$

with the relation given for the interior edges

$$g^S \frac{u_\sigma^{n+1} - u_p^{n+1}}{f(N_p(u^n))\ d_{p\sigma}} + g^S \frac{u_\sigma^{n+1} - u_q^{n+1}}{f(N_q(u^n))\ d_{q\sigma}} = 0, \tag{10}$$

$$\forall \sigma \in \mathcal{E}_{\text{int}} \text{ with } \mathcal{M}_\sigma = \{p, q\},\ \forall n \in \mathbb{N}.$$

Content of the presentation

Estimates on the numerical solution

L^∞ stability of the scheme:

$$|u_p^n| \leq |u_0|_{\mathcal{D},\infty} + |r|_{\mathcal{D},\mathcal{T},\infty}\ T,\ \forall p \in \mathcal{M},\ \forall n = 0, \ldots, \mathbb{N}_T.$$

- This estimate gives us the uniqueness of the numerical solution of the semi-implicit numerical scheme of the studied problem.
- There exists constant ν_S depending only on width of the convolution mask S such that $1 \geq g^S \geq \nu_S > 0$.

Estimates on the numerical solution

$L^2(\Omega \times (0, T))$ estimate on the approximation of the time derivation and $L^\infty(0, T; L^2(\Omega))$ estimate on the approximation of the gradient.

- Non-trivial generalisation of the previous approach had to be done.
- If we define approximation of the function g as it is mentioned in (7) estimate holds only with time and space step of the same order. If we take approximation (8) the stability is unconditioned. The same holds for the theorem on the next slide.
- This estimate leads to the proof of the convergence of the scheme:

Convergence of the scheme

$u_{\mathcal{D}_m,\tau_m}$ defined by $u_{\mathcal{D}_m,\tau_m}(x,t) = u_p^{n+1}$ for a.e. $x \in p$, $\forall t \in (n\tau, (n+1)\tau]$, $\forall p \in \mathcal{M}$, $\forall n \in \mathbb{N}$ tends weakly up to the subsequence to the $\bar{u} \in L^\infty(0,T;H_0^1(\Omega))$, weak solution of the problem (2)-(3)-(4), in $L^2(0,T;H_0^1(\Omega))$.
Moreover if we define:

$$\hat{G}_{\mathcal{D},\tau}(x,t) = \frac{1}{|p|} \sum_{\sigma \in \mathcal{E}_p} (u_\sigma^{n+1} - u_p^{n+1}) n_{p\sigma}, \qquad (11)$$

for a.e. $x \in p$, $t \in (n\tau, (n+1)\tau]$, $\forall p \in \mathcal{M}$, $\forall n \in \mathbb{N}$, it holds that $\hat{G}_{\mathcal{D}_m,\tau_m} \to \nabla \bar{u}$ in $L^2(\Omega \times (0,T))^d$.

Proof will be published soon.

Content of the presentation

1. Introduction to the problem
2. Studied equation and assumptions on the data
3. Theoretical results
4. **Numerical results**
5. Conclusion

Numerical experiments - Object with incomplete border

The goal of the first numerical experiment is to segment the picture showed below:

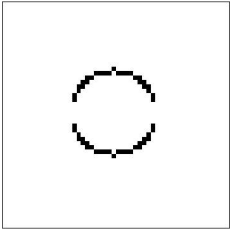

Obr.: Object with incomplete border

Mikula K., Sarti A., Sgallarri A.: *Co-volume method for Riemannian mean curvature flow in subjective surfaces multiscale segmentation* Computing and Visualization in Science, Vol. 9, No. 1, 23-31, 2006.

Numerical experiments - Object with incomplete border

Our method can reconstruct the missing parts of the border of the object. The method is robust against incomplete borders as error in the data.

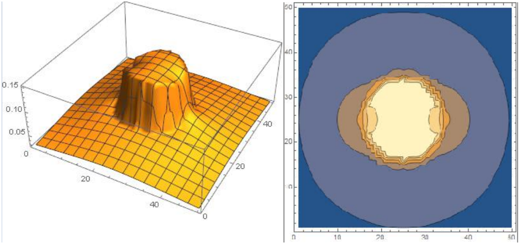

Obr.: Situation after 100 time steps - object with incomplete border

Numerical experiments - Noisy object

Another typical problem with the initial data is noise, so as the second example of the usage of the scheme we chose object below:

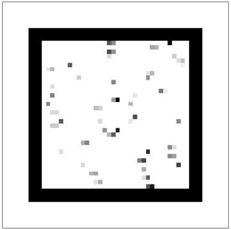

Obr.: Noisy object

Numerical experiments - Noisy object

We can say that noisy data are more time-consuming, but our model and method are robust to the noise as error in the initial data.

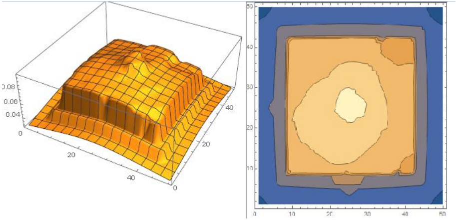

Obr.: Situation after 500 time steps - noisy object

Time dependent 3D segmentation

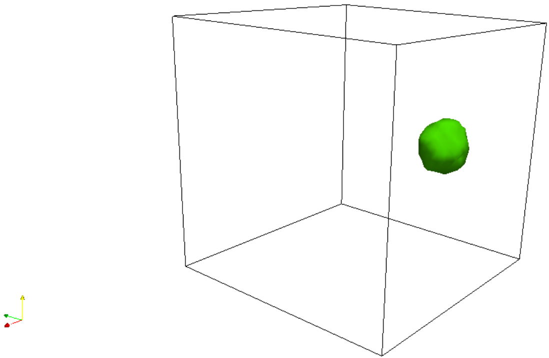

Hornacek T., Mikula K.: Numerical methods for 4D segemntation, STU, 2017.

22/ 27

Time dependent 3D segmentation

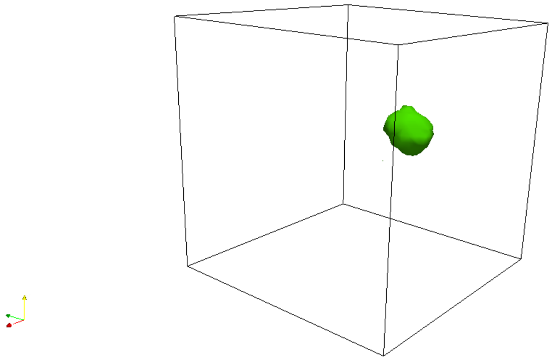

Hornacek T., Mikula K.: Numerical methods for 4D segemntation, STU, 2017.

22/ 27

Time dependent 3D segmentation

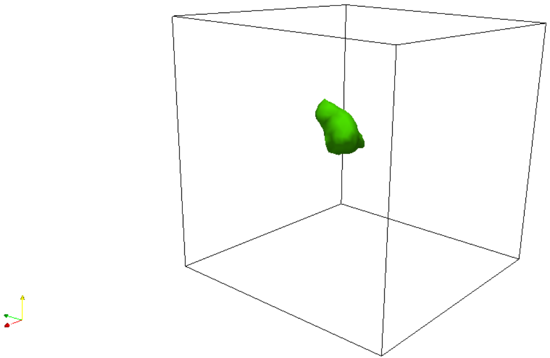

Hornacek T., Mikula K.: Numerical methods for 4D segemntation, STU, 2017.

Time dependent 3D segmentation

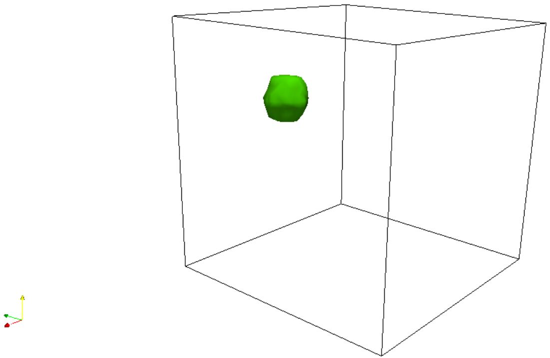

Hornacek T., Mikula K.: Numerical methods for 4D segemntation, STU, 2017.

22/ 27

Time dependent 3D segmentation

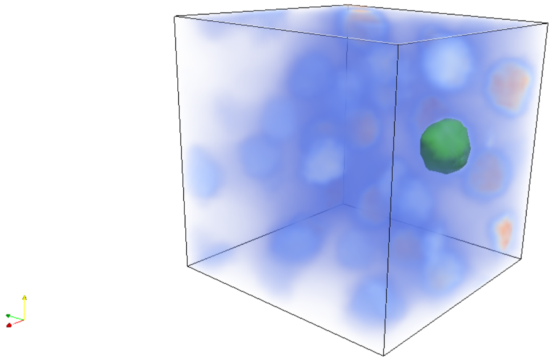

Hornacek T., Mikula K.: Numerical methods for 4D segemntation, STU, 2017.

Time dependent 3D segmentation

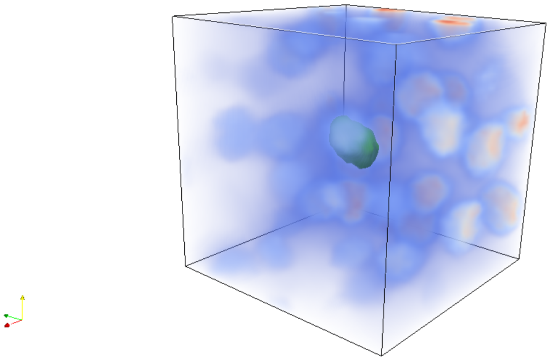

Hornacek T., Mikula K.: Numerical methods for 4D segemntation, STU, 2017.

Time dependent 3D segmentation

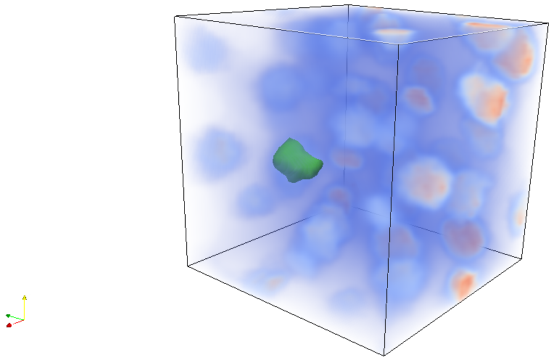

Hornacek T., Mikula K.: Numerical methods for 4D segemntation, STU, 2017.

Time dependent 3D segmentation

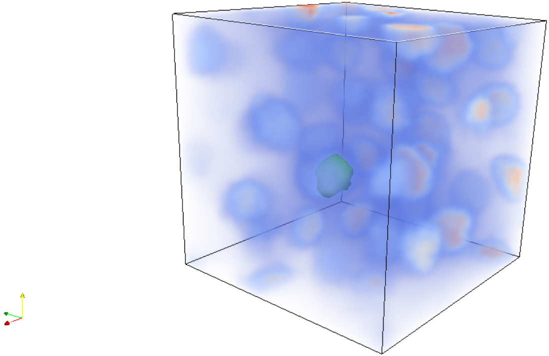

Hornacek T., Mikula K.: Numerical methods for 4D segemntation, STU, 2017.

Time dependent 3D segmentation

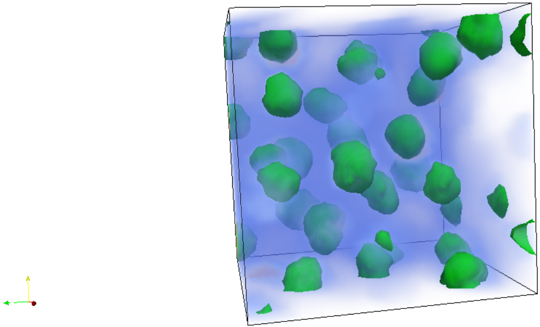

Hornacek T., Mikula K.: Numerical methods for 4D segemntation, STU, 2017.

Time dependent 3D segmentation

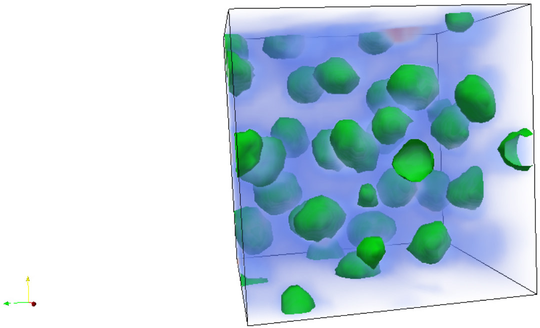

Hornacek T., Mikula K.: Numerical methods for 4D segemntation, STU, 2017.

Time dependent 3D segmentation

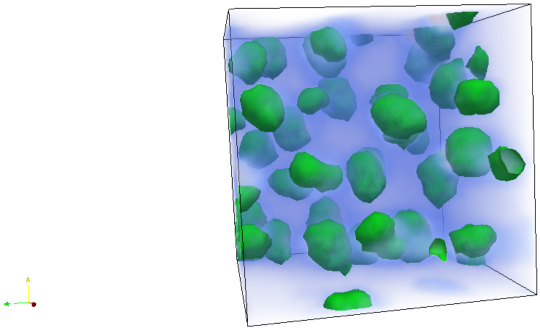

Hornacek T., Mikula K.: Numerical methods for 4D segemntation, STU, 2017.

Time dependent 3D segmentation

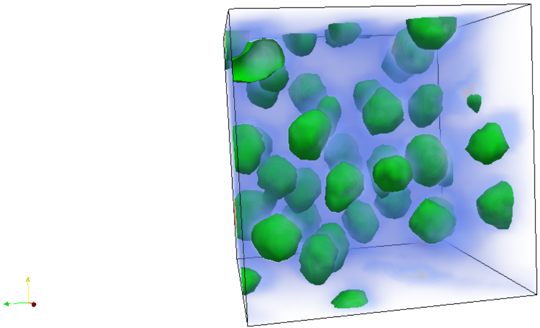

Hornacek T., Mikula K.: Numerical methods for 4D segemntation, STU, 2017.

Time dependent 3D segmentation

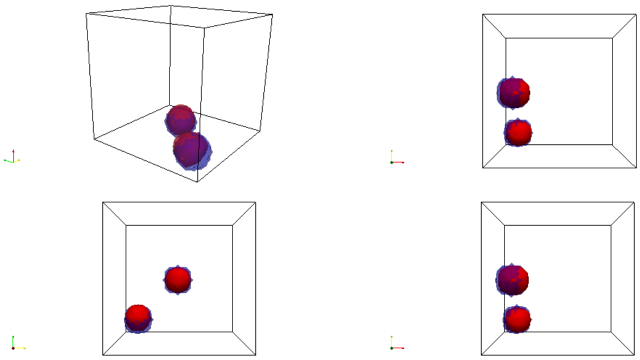

Hornacek T., Mikula K.: Numerical methods for 4D segemntation, STU, 2017.

Time dependent 3D segmentation

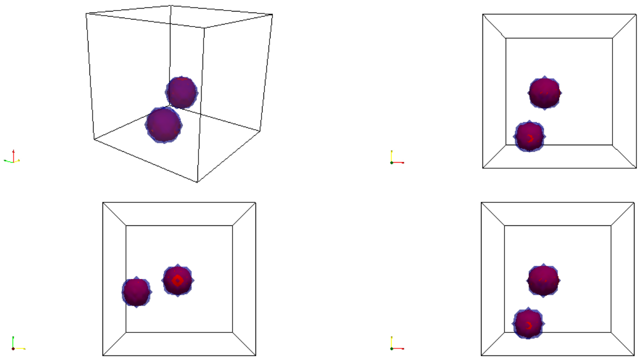

Hornacek T., Mikula K.: Numerical methods for 4D segemntation, STU, 2017.

Time dependent 3D segmentation

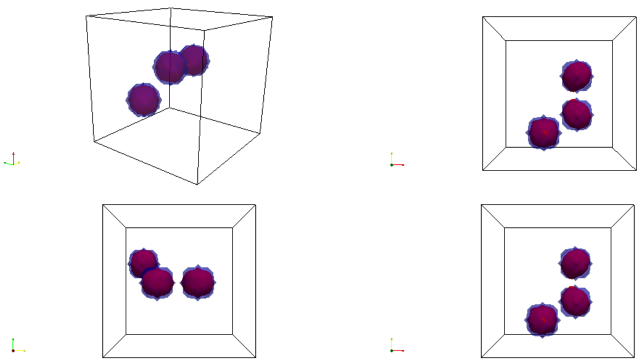

Hornacek T., Mikula K.: Numerical methods for 4D segemntation, STU, 2017.

Time dependent 3D segmentation

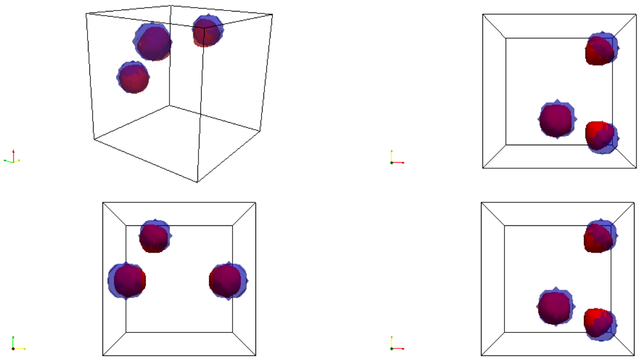

Hornacek T., Mikula K.: Numerical methods for 4D segemntation, STU, 2017.

Content of the presentation

Results

1. New model for image segmentation and edge detection was proposed.

Results

1. New model for image segmentation and edge detection was proposed.
2. Semi-implicit finite volume scheme was constructed.

Results

1. New model for image segmentation and edge detection was proposed.
2. Semi-implicit finite volume scheme was constructed.
3. Existence and uniqueness of the weak solution of the studied problem was proven and convergence of the numerical scheme to this solution was proven as well.

Results

1. New model for image segmentation and edge detection was proposed.
2. Semi-implicit finite volume scheme was constructed.
3. Existence and uniqueness of the weak solution of the studied problem was proven and convergence of the numerical scheme to this solution was proven as well.
4. Numerical tests on the benchmark examples were done.

Results

1. New model for image segmentation and edge detection was proposed.
2. Semi-implicit finite volume scheme was constructed.
3. Existence and uniqueness of the weak solution of the studied problem was proven and convergence of the numerical scheme to this solution was proven as well.
4. Numerical tests on the benchmark examples were done.
5. Model was successfully tested on the real medicine data.